Structural Study on the UCST-Type Phase Separation of Poly(N-isopropylacrylamide) in Ionic Liquid

ARTICLE *in* MACROMOLECULES · FEBRUARY 2013

Impact Factor: 5.8 · DOI: 10.1021/ma3020273

Macromolecules

Article

pubs.acs.org/Macromolecules

Structural Study on the UCST-Type Phase Separation of Poly(*N*-isopropylacrylamide) in Ionic Liquid

Hanako Asai,[†] Kenta Fujii,*[,†] Takeshi Ueki,[‡] Shota Sawamura,[§] Yutaro Nakamura,[§] Yuzo Kitazawa,[§] Masayoshi Watanabe,[§] Young-Soo Han,[∥] Tae-Hwan Kim,[∥] and Mitsuhiro Shibayama*[,†]

[†]Institute for Solid State Physics, The University of Tokyo, Kashiwanoha, Kashiwa, Chiba 277-8581, Japan

[‡]Department of Materials Engineering, Graduate School of Engineering, The University of Tokyo, 7-3-1 Hongo, Bunkyo-ku, Tokyo 113-8656, Japan

[§]Department of Chemistry and Biotechnology, Yokohama National University, 79-5 Tokiwadai, Hodogaya-ku, Yokohama 240-8501, Japan

[∥]Korea Atomic Energy Research Institute, Daejeon, 1045 Daedeok-daero, Yuseong-gu 305-353, Korea

Supporting Information

ABSTRACT: Upper critical solution temperature (UCST)-type phase separation behavior and its conformational change of well-defined poly(*N*-isopropylacrylamide) (pNIPAm) in deuterated room-temperature ionic liquid (IL), 1-ethyl-3-methylimidazolium bis(trifluoromethanesulfonyl)amide (d_8-[C_2mIm$^+$][TFSA$^-$]), were investigated by means of dynamic light scattering (DLS) and small-angle neutron scattering (SANS) measurements. From the temperature dependence of time-averaged scattering intensity obtained by DLS, it was found that the cloud points of pNIPAm/d_8-[C_2mIm$^+$]-[TFSA$^-$] solutions increased with molecular weight (M_w) and concentration. In addition, it was found that there are two relaxation modes of pNIPAm in the IL solutions. From SANS measurements, the radius of gyration, R_g, and the Flory–Huggins interaction parameter, χ, were evaluated as a function of temperature during the phase separation.

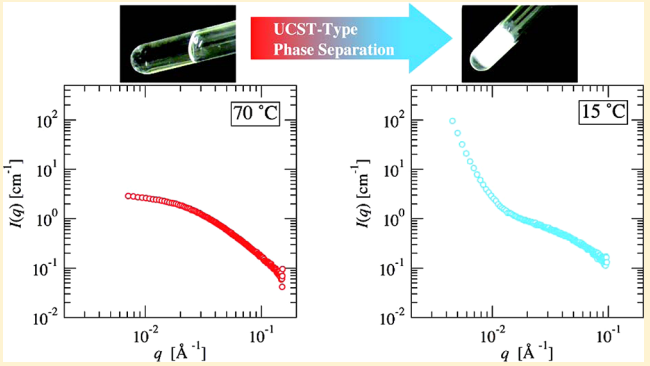

1. INTRODUCTION

Poly(*N*-isopropylacrylamide) (pNIPAm) is a well-known polymer for its lower critical solution temperature (LCST) behavior in water.[1] This characteristic property of pNIPAm aqueous systems has been mainly applied to biomedical fields, such as drug delivery system,[1−5] tissue engineering,[6] cell therapy,[7] and so on. Until today, many researchers have studied the structure of pNIPAm aqueous solutions during phase separation process by differential scanning calorimetry,[8] light scattering,[9,10] small-angle neutron scattering (SANS),[11,12] and so on. For example, Wu et al. have extensively studied the conformational change of pNIPAm by using SANS and dynamic light scattering (DLS) measurements.[10] These pieces of information on temperature dependence of the structure of pNIPAm chain should be a significant insight for the applicational studies.

On the other hand, it is well-known that pNIPAm shows an upper critical solution temperature (UCST) type phase separation behavior in organic solvents or binary (organic solvent–water) mixtures.[13,14] According to the report by Ueki and Watanabe,[15] UCST-type phase separation of pNIPAm was also observed in one of the ionic liquid (IL), 1-ethyl-3-methylimidazolium bis(trifluoromethanesulfonyl)amide ([C_2mIm$^+$][TFSA$^-$]). Because thermosensitive polymer/IL systems have attracted much attention for applications not only to temperature-induced phase transfer systems and micelle shuttle systems,[16,17] but also to thermosensitive self-assembly of block copolymers,[18−20] the detailed information on the structural change of polymer/IL systems also should be essential for these applications. However, there are only a few studies that deal with the temperature dependences of structures of polymers in ILs, except for the SANS and DLS study on the poly(benzyl methacrylate) (pBnMA)/[C_2mIm$^+$]-[TFSA$^-$] solution system, which causes LCST-type phase separation.[21] As for the pBnMA case, the ordered structure formed by the cation–π interaction should play a similar role to the hydrophobic hydration of pNIPAm aqueous solution, resulting in the LCST-type phase behavior. On the other hand, the pNIPAm/[C_2mIm$^+$][TFSA$^-$] system showed a UCST-type phase separation because pNIPAm does not have structural units capable of formation for specific interaction, e.g., cation–π complexation. Considering these differences of

Received: September 26, 2012
Revised: January 19, 2013
Published: January 31, 2013

   dx.doi.org/10.1021/ma3020273 | *Macromolecules* 2013, 46, 1101−1106

phase separation difference, the structural change during phase separation of the pNIPAm/[C_2mIm$^+$][TFSA$^-$] system should differ from that of the pBnMA/[C_2mIm$^+$][TFSA$^-$] system.

In this study, we investigated the UCST-type phase separation of well-defined pNIPAm in [C_2mIm$^+$][TFSA$^-$] in terms of structural viewpoints. SANS and DLS experiments were performed for pNIPAm/IL solutions with various molecular weights (M_w) and concentrations. From the experimental data, we discuss the characteristics of the phase separation of pNIPAm/[C_2mIm$^+$][TFSA$^-$] system compared with the cases of pNIPAm/water system and pBnMA/[C_2mIm$^+$][TFSA$^-$] system.

2. EXPERIMENTAL SECTION

2.1. Materials. Partially deuterated ionic liquid (d_8-[C_2mIm$^+$][TFSA$^-$]) and *S*-1-dodecyl-*S*′-(α,α′-dimethyl-α″-acetic acid) trithiocarbonate (CTA) were synthesized and characterized according to the procedures reported earlier.[22−24] 1-Dodecanethiol, acetone (dehydrated), and carbon disulfide were purchased from Kanto Chemical. 2,2-Azobis(isobutyronitrile) (AIBN) and Aliquat 336 were from Sigma-Aldrich. NIPAm was generously provided by the Kojin Corporation and purified by recrystallization (two times) using a toluene/hexane (1:10 by weight) mixed solvent. AIBN was recrystallized from methanol prior to use. All other chemical reagents were used as received, unless otherwise noted. As is well-known, the deuteration for solvent affects the phase separation behavior, particularly the cloud point.[10,25] In this work, therefore, we used only deuterated ILs as a solvent for both SANS and DLS including transmission measurements.

2.2. Preparation of pNIPAm. The pNIPAms having different M_ws were prepared by well-established reversible addition−fragmentation chain transfer (RAFT) polymerization. Here, we describe a representative synthetic procedure for pNIPAm (24 kDa). 0.0365 g of CTA (0.10 mmol) and 5.55 g of NIPAm (49.1 mmol) were dissolved in 60 mL of 1,4-dioxane at 45 °C. A total of 0.0102 g of AIBN (0.062 mmol) was separately dissolved in 10.2 mL of 1,4-dioxane in another round-bottom flask and dearated by purging N_2 for 30 min at room temperature. A total of 3.3 mL of AIBN solution (0.020 mmol) was then added to the monomer solution. RAFT polymerization was carried out at 65 °C for 24 h. The products were evaporated and purified by reprecipitation three times from acetone as a good solvent and cold diethyl ether as a poor solvent.

Following RAFT polymerization and purification, the dodecyl trithiocarbonate residue derived from CTA attached to the polymer (pNIPAm-CTA) terminus was removed according to the following procedure in order to avoid undesirable aggregation of pNIPAm in an IL due to intermolecular interaction with terminal residues. A total of 3.4 g of pNIPAm-CTA (0.1 mmol) and 0.492 g of AIBN (3.0 mmol) was dissolved in 80 mL of ethanol. The solution was deaerated by purging N_2 for 30 min at room temperature. The cleavage reaction was carried out at 80 °C for 12 h under a N_2 atmosphere. The product was evaporated and purified by reprecipitation three times from acetone as a good solvent and cold diethyl ether as a poor solvent. All polymers were characterized by ^{1}H NMR. The number-average molecular weight (M_n) and polydispersity index (M_w/M_n) of the polymers were determined by gel permeation chromatography (GPC) using dimethylformamide (DMF) containing 0.01 mol L^{-1} LiBr as the carrier solvent. The columns (Tosoh, Co. Ltd., Japan) for the GPC were calibrated using polystyrene standards. The polydispersity indices of all three polymers were relatively narrow (<1.2).

2.3. Dynamic Light Scattering (DLS) Simultaneous Transmission Measurement. DLS and simultaneous transmission measurements for pNIPAm solutions were carried out using DLS/SLS-5000 compact goniometer (ALV, Langen, Germany), coupled with an ALV photon correlator. The sample concentrations were 1, 3, and 5 wt % for both 24 and 100 kDa pNIPAm/IL solutions. We synthesized the IL by ourselves, and the optical purity was confirmed to be high enough. Therefore, we skipped the filteration. This was advantageous to check the existence of clustering structures, which are often observed in aqueous polymer solutions.[26] A 22 mW helium−neon laser (wavelength, λ = 632.8 nm) was used as incident beam, and the scattering angle θ was 90°. As decreasing temperature from 70 °C to the cloud point, DLS data were obtained every 40 s (the measurement time was 30 s at intervals of 10 s). The measurement temperature was monitored at the sample position by a thermocouple. The time−intensity correlation functions were converted to the distribution functions with CONTIN (the constrained regularization method).[27] Note that the DLS measurement could not be carried out for completely phase-separated opaque samples because of multiple scattering.

2.4. Viscosity Measurement. For quantitative data analysis of DLS experiments, temperature and concentration dependences of the viscosity, η, of pNIPAm/[C_2mIm$^+$][TFSA$^-$] solutions were measured by using a rheometer (MCR501, Anton Paar, Austria) with a cone−plate geometry. The obtained η_0s were plotted against temperature and numerically fitted with the function $\eta_0 = 3.02 + 58.3 \exp(-0.0295T)$, where η_0 is viscosity of the neat IL in cP unit and T is the measurement temperature in the Celsius temperature unit.

2.5. Refractive Index Measurement. The temperature dependence of the refractive index, n, of neat [C_2mIm$^+$][TFSA$^-$] (solvent) was measured by an Abbe refractometer (Atago, Japan) attached to a thermostat bath. The measurements were carried out on nondeuterated IL at 20, 25, 30, 40, 50, and 60 °C. The obtained temperature dependence of refractive indices was numerically fitted with the function $n = -2.76 \times 10^{-4}T + 1.43$. The calculated n values from this function were similar to those reported previously.[28] We used the n values estimated from this equation for the DLS analysis. Here, we assumed the refractive index of the deuterated IL was the same as nondeuterated IL.

2.6. Small-Angle Neutron Scattering (SANS). SANS experiments were carried out on High-flux Advanced Neutron Application Reactor (HANARO) located at Korea Atomic Energy Research Institute (KAERI), Korea.[29] A monochromated cold neutron beam with an average neutron wavelength 6.00 Å was irradiated to the samples. The scattered neutrons were counted with a 2D detector. The sample concentrations were the same as the DLS experiment, i.e., 1, 3, and 5 wt % for both 24 and 100 kDa pNIPAm/the d_8-[C_2mIm$^+$][TFSA$^-$] solutions. The sample-to-detector distance (SDD) was chosen to be 7 m for all the 24 kDa samples, 1 wt % 100 kDa samples, and the other samples above 40 °C, while 11 m for the other cases. After necessary corrections for open beam scattering, transmission, and detector inhomogeneities, the corrected scattering intensity functions were normalized to the absolute intensity scale.

3. RESULTS AND DISCUSSION

3.1. Transmission Measurements and Determination of Chain-Overlap Concentration (c^*). Figure 1 shows the

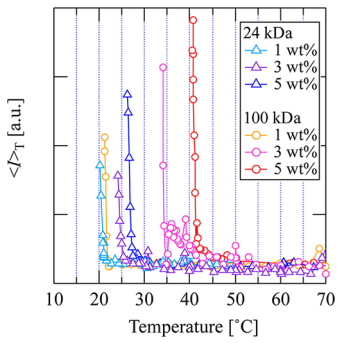

Figure 1. Temperature dependence of time-averaged scattering intensities, $\langle I \rangle_T$s, of pNIPAm/IL solutions with various concentrations and M_ws. At each cloud point, $\langle I \rangle_T$ steeply increased, indicating that the solution changed from transparent to turbid by UCST-type phase separation.

dx.doi.org/10.1021/ma3020273 | Macromolecules 2013, 46, 1101−1106

temperature dependence of time-averaged light scattering intensities, $\langle I \rangle_T$, for the pNIPAm/IL solutions with various M_w and concentration of polymer. As shown in this figure, $\langle I \rangle_T$ drastically increased with decreasing temperature, indicating the pNIPAm/IL solution changes from transparent to turbid (cloud point). Thus, obtained cloud points are plotted in Figure 2 as a function of pNIPAm concentration and M_w. The

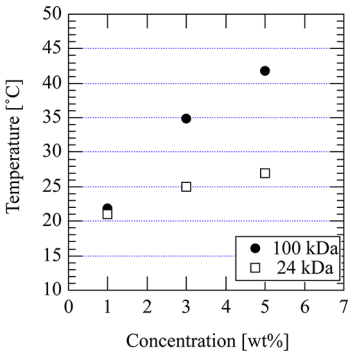

Figure 2. Concentration and M_w dependence of the cloud point of pNIPAm/IL solutions. Phase separation occurs below the cloud point.

cloud points were dependent on the pNIPAm concentration and M_w as previously reported.[15] This behavior can be explained by Flory–Huggins theory and is commonly observed in polymer solution system.[30] However, it is not the case for the pNIPAm aqueous solution, where rather a constant cloud point temperature is observed irrespective of concentrations and M_w.[25] In the following section, we will show structural change of pNIPAm in the IL and discuss the difference between IL and aqueous solution systems.

Before discussing DLS and SANS results, we evaluated the chain-overlap concentration (c^*) from viscosity measurements via the equation

$$c^* = \frac{3 \times 6^{3/2}\Phi}{4\pi N_A [\eta]} \quad (1)$$

where Φ is the universal constant, and we employed the value of $\Phi = 2.1 \times 10^{23}$.[31] The intrinsic viscosities, $[\eta]$s, were determined by extrapolating η_{red} to $c = 0$ (not shown here). Here, c is the polymer concentration and η_{red} is the reduced viscosity. The c^* values at 70 °C were 6.3 and 2.6 wt % for 24 and 100 kDa, respectively. Considering thus-obtained c^* values, it was conjectured that the all of the 24 kDa samples used for SANS and DLS experiments were in dilute regime, while the 100 kDa samples except 1 wt % were in semidilute regime.

3.2. DLS. Figure 3 shows the temperature dependence of (a) the intensity correlation functions and (b) the hydrodynamic radius (R_h) distribution functions obtained by DLS measurements for 3 wt % 24 kDa pNIPAm solutions, which is in dilute regime. The linear–log plot of Figure 3a is shown in Figure S1. As shown in Figure 3a, there are two relaxation modes in high temperature region, but only one relaxation was observed below the cloud point (in this case 25 °C). These results also can be seen in the R_h distribution functions in Figure 3b, which were obtained from the inverse-Laplase transform of the correlation functions. There are two distinct peaks at around 70 °C in Figure 3b. The left side peak corresponds to molecularly dissolved pNIPAm chains with a few nanometers size. The right side peak, on the other hand, corresponds to clustered pNIPAm chains. It should be noted that the fraction of the large clusters

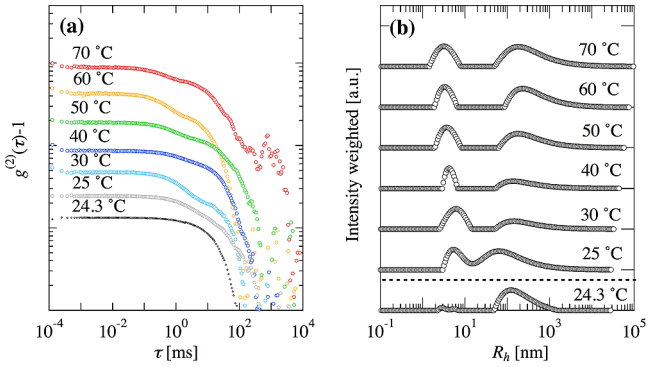

Figure 3. Typical results of (a) intensity correlation functions and (b) R_h distributions for 24 kDa 3 wt % pNIPAm/IL solution at various temperatures. The correlation functions in part (a) are vertically shifted to see easily. The broken line in part (b) indicates the phase separation boundaries, 25.0 °C.

is less than 1 wt % according to the estimation based on the previous paper.[32] This is because that the peak intensity is emphasized by the factor of the sixth power of the size ratio of the individual polymer chains to the clusters, i.e., $(R_{h,cluster}/R_{h,chain})^6$, due to the nature of scattering. Hence, it can be conjectured that there coexist two states in the high-temperature region: one being a molecular dispersion and the other clustered chains, and the former is dominant. As temperature decreases, the both peaks move closer to each other. The shift of the right peak to the left is ascribed to shrinkage of the cluster due to lowering of the solvent quality. On the other hand, the left side peak shifted to the right. The right-side shift indicates the chains expand even though the lowering of the solvent quality. Finally, a single peak appears below the cloud point (the broken line in Figure 3b) as a result of marging the two peaks. This single peak corresponds to large clusters (submicrometer size) and indicates that a UCST phase separation occurred.

It should be noted that this structural change in the IL solution is rather gradual with respect to temperature in comparison with that in aqueous solution system, where a drastic structural change occurs at LCST.[33] Other dilute IL solutions also show a similar behavior to Figure 3, and the temperature dependence of R_h values, corresponding to the left side peaks, are shown in Figure S2.

3.3. SANS Analysis. Figure 4 shows SANS profiles observed for (a) 24 kDa and (b) 100 kDa pNIPAm in deuterated IL, i.e., d_8-[C_2mIm$^+$][TFSA$^-$] (3 wt % pNIPAm concentration). The SANS intensity gradually increased with decreasing temperature for all the systems, and then large upturns were observed at 15 and 25 °C for 24 and 100 kDa solutions, respectively. Here, the SANS curve at low q is scaled with $I(q) \sim q^{-4}$. Interestingly, the temperatures at which the steep upturn in $I(q)$ occurred were ca. 10 °C lower than the cloud points determined by DLS for both 100 and 24 kDa samples (see Figure 2). Note that the SANS samples became opaque at 25 °C for 3 wt % 24 kDa sample and at 35 °C for 3 wt % 100 kDa sample as shown with an arrow in Figuire 4. Hence, the two temperatures, i.e., the upturn temperature and the opaque temperature, were not consistent in this system. A similar phenomenon was also observed in the case of pBnMA/d_8-[C_2mIm$^+$][TFSA$^-$] solutions, although the phase separation behavior was opposite (i.e., LCST).[21] On the other hand, large upturns in SANS were observed only in the low-q regions while

dx.doi.org/10.1021/ma3020273 | Macromolecules 2013, 46, 1101–1106

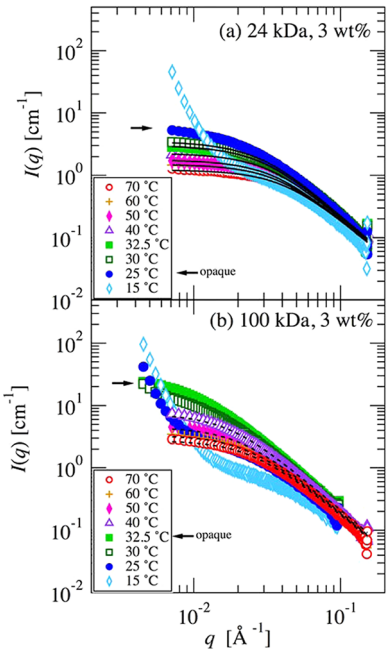

Figure 4. Temperature dependence of SANS profiles for 3 wt % pNIPAm/IL solution: (a) 24 kDa and (b) 100 kDa. The solid black lines and the broken lines indicate the fitting results by eqs 3 and 5, respectively.

there remain $I(q) \sim q^{-2}$ in the high-q regions for both IL systems of pNIPAm and pBnMA. These results indicate that there should exist both large aggregates and individual chains in the IL solutions after complete phase separations. In pNIPAm aqueous solutions, the cloud points correspond to the temperature where the $I(q) \sim q^{-4}$ is observed in the SANS profiles.[12] According to our previous paper on pBnMA/the IL system, the intermediate temperature region was attributed to the presence of pre-phase separation. The detailed mechanism of this phenomenon will be reported by studying the solvation structure of the IL system. In this study, we restrict our discussion on the chain structures before the phase separation (i.e., above cloud points), and the structures after phase separation will be explored in a forthcoming paper.

At first, we carried out SANS analysis for dilute 24 kDa solutions by using a Zimm plot. At the limit of low concentration and low q, $I(q)$ can be described in terms of the following Zimm equation

$$\frac{Kc}{I(q)} = M_w^{-1}\left(1 + \frac{R_g^2}{3}q^2\right) + 2A_2c \tag{2}$$

where $K = \Delta\rho^2 N_A/d_{pNIPAm}^2$ (for the present case, $K = 0.0018$ mol cm^2 g^{-2}) is the contrast factor ($\Delta\rho$ is the difference of scattering length densities between pNIPAm and the IL (i.e., 3.568×10^{10} cm^{-2}), and d_{pNIPAm} is the mass density of the pNIPAm), N_A is the Avogadro's number, R_g is the radius of gyration, and A_2 is the second virial coefficient accounting for the molecular interactions between pNIPAm chains. Figure 5 shows the Zimm plots for 70−30 °C. According to eq 2, we successfully obtained reasonable values of M_ws for pNIPAm (the average M_w value is 24.0 kDa), confirming the validity of the experiment and the analysis. Note that the slope of A_2, the concentration dependence, i.e., changes its sign between 50 and 40 °C as shown in the figure. Figure 6 shows the temperature dependence of (a) R_g at $c \to 0$ and (b) A_2, which are also obtained from the Zimm plot. As shown in Figure 6a, the R_g values for the dilute 24 kDa solutions and the A_2 value became smaller as decreasing temperature and the A_2 value became negative at the temperatures around 45 °C (≈ the Θ temperature).

Note that because the Zimm plot is valid only for the dilute solutions, only the 24 kDa solutions are appropriate for the

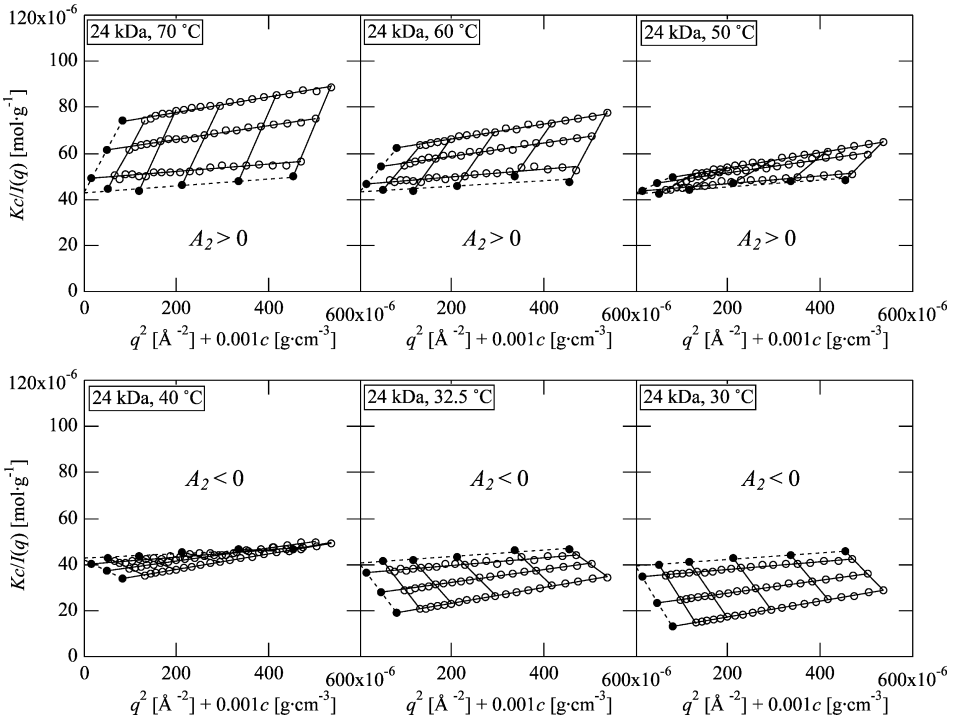

Figure 5. Zimm plot for 24 kDa pNIPAm/the IL solutions for various temperatures.

dx.doi.org/10.1021/ma3020273 | Macromolecules 2013, 46, 1101−1106

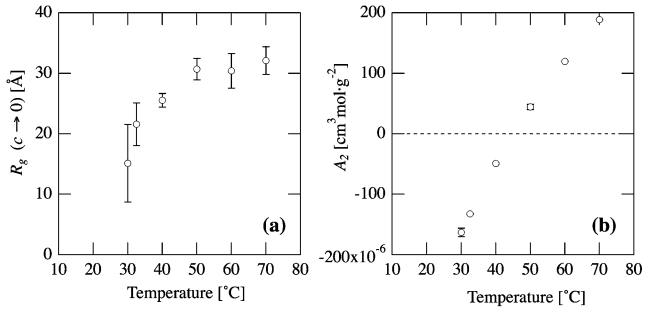

Figure 6. (a) Temperature dependence of the radius of gyration (R_g) at $c \to 0$ and (b) the second virial coefficient (A_2), obtained from the Zimm plot for 24 kDa samples shown in Figure 5.

Zimm plot. Next, we carried out the curve fitting analysis for all the observed profiles above the cloud point. Considering the polymer concentrations, we used the following Debye function (eqs 3 and 4) and Ornstein−Zernike function (eq 5) as fitting functions for dilute samples (i.e., 24 kDa samples and 100 kDa 1 wt %) and semidilute samples (i.e., the other 100 kDa samples), respectively.

$$I(q) = \frac{(\Delta\rho)^2}{N_A} \frac{V_2 \phi P_D(q)}{1 + (1 - 2\chi)\left(\frac{V_2}{V_1}\right)\phi P_D(q)} \quad (3)$$

$$P_D(q) = Z\frac{2}{u^2}(e^{-u} - 1 + u), \qquad u = R_g{}^2 q^2 \quad (4)$$

$$I(q) = \frac{(\Delta\rho)^2 RT\phi^2}{N_A K_{os}} \frac{1}{1 + q^2\xi^2} \quad (5)$$

Here, χ is the Flory−Huggins's interaction parameter, ϕ is the polymer volume fraction, Z is the degree of polymerization, ξ is the correlation length, K_{os} is the osmotic modulus, and V_1 and V_2 are the molar volumes of the IL and pNIPAm, respectively. Equations 3 and 5 are well-known scattering functions to describe polymer chains in dilute and semidilute solution state, respectively.[34,35] The observed $I(q)$s are well reproduced by both eqs 3 and 5, as shown with solid black lines and broken lines in Figure 4, respectively.

Figure 7 shows (a) R_g, (b) ξ, and (c) χ values obtained from the fitting analysis as a function of temperature. It was found in Figure 7a that the R_g values became smaller as decreasing temperature, indicating that the pNIPAm chains gradually shrink with approaching the cloud points. Here, it should be noted that the temperature dependence for R_g values was opposite to that for the R_h values (Figure S2). We conjecture the physical meaning of this opposite R_g and R_h behavior as following: Considering the temperature dependence of R_g/R_h ratio (Figure S3), which provides the information about the chain comformation, it is found that the R_g/R_h ratio decreased toward each of the cloud point from ca. 1.5 to 0.5, although data points of 24 kDa 1 wt % and 100 kDa 1 wt % are somewhat larger due to experimental error or some other reasons. This decrease of R_g/R_h ratio is ascribed to the crossover of the temperature dependences of R_h and R_g and indicates that the chain conformation changes from random coil to hard sphere state.[36]

The ξ values of semidilute 100 kDa samples shown in Figure 7b become larger as decreasing temperature. This indicates an enhancement of concentration fluctuations by approaching the cloud point. The ξ values decrease at high temperatures as

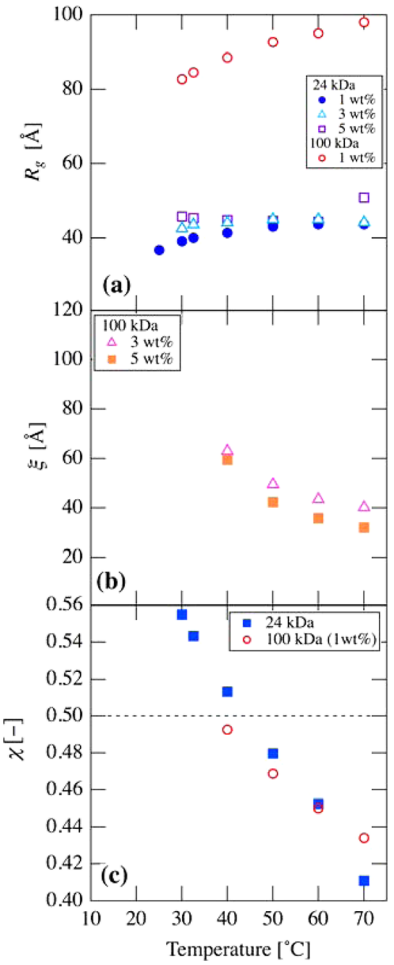

Figure 7. Temperature dependence of (a) R_g, (b) ξ, and (c) χ obtained from curve fittings shown in Figure 4. In part (c), the χ values of 100 kDa are evaluated only from 1 wt % solutions, which are fitted by Debye function, in the same way as 24 kDa samples. The solid line indicates $\chi = 0.5$.

increasing concentration, which is a well-known behavior for semidilute polymer solutions in a good solvent. In Figure 7c, it can be seen that the χ parameter becomes smaller with increasing temperature and approaches 0.5 at around 45 °C for 24 kDa, suggesting that the Θ temperature in this system is ca. 45 °C, which is in good agreement with the result shown in Figure 7b. However, the Θ temperature for 100 kDa is lower than that estimated from 24 kDa. One of the possible reasons is the effect of flexibility of pNIPAm chain, considering that the χ parameter should be constant for a theoretical stiff polymer.[37]

4. CONCLUSION

The nanoscale structural change during the UCST-type phase separation process of poly(*N*-isopropylacrysamide)/d_8-1-ethyl-3-methylimidazolium bis(trifluoromethanesulfonyl)amide (pNIPAm/d_8-[C_2mIm$^+$][TFSA$^-$]) solutions with two molecular weights (M_w) and various concentrations was investigated as a function of temperature by means of dynamic light scattering (DLS) and small-angle neutron scattering (SANS) measurements. From the temperature dependence of time-averaged scattering intensity obtained by DLS, it was found that the cloud points of pNIPAm/IL solutions increased with M_w and concentration. From SANS measurements, the radius of gyration, R_g, and the correlation length, ξ, were quantitatively

dx.doi.org/10.1021/ma3020273 | *Macromolecules* 2013, 46, 1101−1106

evaluated. The R_g values (for $c < c^*$) decreased, while ξ values (for $c > c^*$) increased as approaching UCST. The Flory–Huggins interaction parameter, χ, became larger as decreasing temperature, and it exceeded 0.5 around 45 °C ($\approx$ the Θ temperature). Similar to the case of pBnMA/IL, molecularly dispersed pNIPAm chains still remain after macroscopic phase sepraration, which is a marked difference from aqueous pNIPAm sysetems.

■ ASSOCIATED CONTENT

Supporting Information

Linear–log plot of correlation functions of 24 kDa 3 wt % pNIPAm/$[C_2mIm^+][TFSA^-]$ solution with various temperatures; temperature dependences of the R_h values (fast modes) for the dilute samples; temperature dependences of the R_g/R_h ratios. This material is available free of charge via the Internet at http://pubs.acs.org.

■ AUTHOR INFORMATION

Corresponding Author

*E-mail shibayama@issp.u-tokyo.ac.jp; k-fujii@issp.u-tokyo.ac.jp.

Notes

The authors declare no competing financial interest.

■ ACKNOWLEDGMENTS

This work has been financially supported by Grant-in-Aids for Scientific Research from the Ministry of Education, Culture, Sports, Science and Technology (No. 24750066 to K.F., No. 22245018 to M.S., No. 23245046 to M.W.), and Research Fellowship of the Japan Society for the Promotion of Science for Young Scientists (No.11J07791 to T.U.). The SANS experiment was performed by using 40 m SANS at HANARO, KAERI, Daejeon, South Korea and also by SANS-U at JRR-3 with the approval of Institute for Solid State Physics, The University of Tokyo (proposal no. 11581), Japan Atomic Energy Agency, Tokai, Japan.

■ REFERENCES

(1) Schild, H. G. *Prog. Polym. Sci.* **1992**, *17*, 163–249.
(2) Hoffman, A. S.; Afrassiabi, A.; Dong, L. C. *J. Controlled Release* **1986**, *4*, 213–222.
(3) Wei, H.; Cheng, S.-X.; Zhang, X.-Z.; Zhuo, R.-X. *Prog. Polym. Sci.* **2009**, *34*, 893–910.
(4) Nakayama, M.; Okano, T.; Miyazaki, T.; Kohori, F.; Sakai, K.; Yokoyama, M. *J. Controlled Release* **2006**, *115*, 46–56.
(5) Piskin, E. *Int. J. Pharm.* **2004**, *277*, 105–118.
(6) Wu, J.-Y.; Liu, S.-Q.; Heng, P. W.-S.; Yang, Y.-Y. *J. Controlled Release* **2005**, *102*, 361–372.
(7) Cho, J. H.; Kim, S.-H.; Park, K. D.; Jung, M. C.; Yang, W. I.; Han, S. W.; Noh, J. Y.; Lee, J. W. *Biomaterials* **2004**, *25*, 5743–5751.
(8) Shibayama, M.; Suetoh, Y.; Nomura, S. *Macromolecules* **1996**, *29*, 6966–6968.
(9) Kazakov, S. V.; Galaev, I. Y.; Mattiasson, B. *Int. J. Thermophys.* **2002**, *23*, 161–173.
(10) Wang, X.; Wu, C. *Macromolecules* **1999**, *32* (13), 4299–4301.
(11) Shibayama, M.; Isono, K.; Okabe, S.; Karino, T.; Nagao, M. *Macromolecules* **2004**, *37*, 2909–2918.
(12) Meier-Koll, A.; Pipich, V.; Busch, P.; Papadakis, C. M.; Muller-Buschbaum, P. *Langmuir* **2012**, *28*, 8791–8798.
(13) Koyama, M.; Hirano, T.; Ohno, K.; Katsumoto, Y. *J. Phys. Chem. B* **2008**, *112*, 10854–10860.
(14) Yamauchi, H.; Maeda, Y. *J. Phys. Chem. B* **2007**, *111*, 12964–12968.
(15) Ueki, T.; Watanabe, M. *Chem. Lett.* **2006**, *35*, 964.
(16) Horton, J. M.; Bai, Z.; Jiang, X.; Li, D.; Lodge, T. P.; Zhao, B. *Langmuir* **2011**, *27*, 2019–2027.
(17) Bai, Z.; Lodge, T. P. *Langmuir* **2010**, *26*, 8887–8892.
(18) Ueki, T.; Watanabe, M.; Lodge, T. P. *Macromolecules* **2009**, *42*, 1315–1320.
(19) He, Y.; Lodge, T. P. *Chem. Commun.* **2007**, 2732–2734.
(20) Kitazawa, Y.; Ueki, T.; Niitsuma, K.; Imaizumi, S.; Lodge, T. P.; Watanabe, M. *Soft Matter* **2012**, *8*, 8067–8074.
(21) Fujii, K.; Ueki, T.; Niitsuma, K.; Matsunaga, T.; Watanabe, M.; Shibayama, M. *Polymer* **2011**, *52*, 1589–1595.
(22) Fujii, K.; Asai, H.; Ueki, T.; Sakai, T.; Imaizumi, S.; Chung, U.; Watanabe, M.; Shibayama, M. *Soft Matter* **2012**, *8* (6), 1756–1759.
(23) Rzayev, J.; Hilmyer, M. A. *J. Am. Chem. Soc.* **2005**, *127*, 13373–13379.
(24) Lai, J. T.; Filla, D.; Shea, R. *Macromolecules* **2002**, *35*, 6754–6756.
(25) de Azevedo, R. G.; Rebelo, L. P. N.; Ramos, A. M.; Szydlowski, J.; de Sousa, H. C.; Klein, J. *Fluid Phase Equilib.* **2001**, *185*, 189–198.
(26) Polverari, M.; van de Ven, T. G. M. *J. Phys. Chem.* **1996**, *100*, 13687–13695.
(27) Provencher, S. W. *Comput. Phys. Commun.* **1982**, *27*, 213–227.
(28) Ueki, T.; Karino, T.; Kobayashi, Y.; Shibayama, M.; Watanabe, M. *J. Phys. Chem. B* **2007**, *111*, 4750–4754.
(29) Han, Y. S.; Choi, S. M.; Kim, T. H.; Lee, C. H.; Kim, H. R. *Physica B* **2006**, *385–386*, 1177–1179.
(30) Shultz, A. R.; Flory, P. J. *J. Am. Chem. Soc.* **1952**, *74*, 4760–4767.
(31) Fujita, H. *Polymer Solution*; Elsevier: Amsterdam, 1990.
(32) Shibayama, M.; Karino, T.; Okabe, S. *Polymer* **2006**, *47*, 6446–6456.
(33) Reddy, P. M.; Taha, M.; Venkatesu, P.; Kumar, A.; Lee, M.-J. *J. Chem. Phys.* **2012**, *136*, 234904.
(34) Shibayama, M. Small-angle Neutron Scattering on Gels. In *Soft Matter Characterization*; Pecora, P., Borsali, R., Eds.; Springer-Verlag: Berlin, 2008; Vol. 2, pp 783–832.
(35) Hammouda, B.; Nakatani, A. I.; Waldow, D. A.; Han, C. C. *Macromolecules* **1992**, *25*, 2903–2906.
(36) Wu, C.; Zhou, S. *Macromolecules* **1995**, *28*, 8381.
(37) Murakami, H.; Norisuye, T.; Fujita, H. *Macromolecules* **1980**, *13*, 345–352.